Analysis of noise generated by a wall mounted finite-length airfoil

Narasimha M. Thota, Laura A. Brooks, Danielle J. Moreau, Anthony C. Zander and Con J. Doolan

School of Mechanical Engineering, The University of Adelaide, Adelaide, South Australia, 5005, Australia

ABSTRACT

In order to produce aircraft, turbo-machinery and helicopters with low acoustic signatures and without annoying tones, it is essential to understand the noise generated by airfoils. A series of experiments were carried out in the anechoic wind tunnel facility at the University of Adelaide with subsonic, low Mach number turbulent flow over a wall-mounted finite-length NACA 0012 airfoil of span 124 mm and chord 67 mm (aspect ratio of 1.851). Acoustic data were acquired using two phase-matched microphones, one mounted 560 mm above and the other 560 mm below the trailing edge of the airfoil, for flow conditions in the Reynolds number range of 2.2×10^4 - 1.675×10^5. Experiments were conducted for airfoil geometric angles of attack (α) of 0º, 5º and 10º. From the experimental measurements, it is evident that the noise spectra contained broadband noise together with tonal components of various frequencies and sound pressure levels. In this paper, the effect of the airfoil tip on its tonal noise behavior and the effects of Reynolds number and angle of attack on the far-field noise radiated from the airfoil are presented and compared with experimental and numerical investigations carried out by others for similar geometries and flow conditions.

INTRODUCTION

Understanding how airfoils create tonal noise at low-to-moderate Reynolds numbers is very important as under current legislation, tones are objectionable in the commercial aircraft industry (Smith, 1989, DOT/FAA, 1990). Tonal noise emanating from wind turbines may also seriously annoy residents living close by (Doolan, 2008). Therefore, for any engineering application of airfoils, researchers mainly aim at eliminating the tones above certain EPNLdB (Effective Perceived Noise Level in dB) and reducing broadband noise.

Paterson et al. (1973) tested three isolated airfoils (two 2-D airfoils: NACA 0012, NACA 0018 and one 3-D NACA 0012 airfoil) at low Reynolds numbers and measured far-field noise, surface pressure fluctuations and their correlation coefficients. They have proposed vortex shedding at the trailing edge as the mechanism for the generation of tonal noise and also devised a frequency scaling law for the primary tones. Tam (1974) disagreed with the theory proposed by Paterson et al. (1973) and suggested that the generation of tones is due to a self excited aero-acoustic feedback loop. Both Paterson et al. (1973) and Tam (1974) supported their theories with experimental results. Arbey et al. (1983) conducted experimental investigations using a 2-D airfoil of NACA 0012 section at low Reynolds numbers and observed that the far field acoustic spectrum was comprised of broadband noise overlapped with a primary tone and equidistant narrow band peaks. They also suggested that tonal noise and its frequency selection were due to a feedback loop mechanism caused by the diffraction of the Tollmein-Schlichting (T-S) waves at the trailing edge, as originally proposed by Tam (1974). Nash et al. (1999) tested a NACA 0012 airfoil, both numerically and experimentally, at low Reynolds numbers. They proposed a new mechanism for tonal noise generation and its frequency selection based on the growth of T-S instability waves.

Desquenses et al. (2007) investigated the noise generated by a 2-dimensional NACA 0012 airfoil, using direct numerical simulation (DNS). They presented plots of angle of attack versus Reynolds number, with identifiable zones where tones are and are not produced. Their observations were in good agreement with the results of Paterson et al. (1973) and Nash et al. (1999). Kingan et al. (2009) has developed an accurate and robust theoretical model for predicting the tonal frequencies and validated their model against the results obtained from experiments. Arcondoulis et al. (2009) presented similar research for a NACA 0012 airfoil.

The present authors have carried out experimental investigation on a finite length airfoil (aspect ratio 1.851) at low-to-moderate Reynolds numbers ($2.2 \times 10^4 < Re_c < 1.675 \times 10^5$) and three geometric angles of attack (α = 0º, 5º and 10º), to understand not just the trailing edge noise, but also noise radiated by the leading edge and the tip. Most importantly, the authors aim to study tip effects on the tonal behavior of the airfoil. However, the present paper outlines preliminary investigations into understanding the overall finite length airfoil noise by comparing it with a full-span airfoil in order to understand the major differences between the overall noise spectra.

EXPERIMENTAL SETUP AND EQUIPMENT USED

Experiments were conducted in the anechoic wind tunnel (AWT) facility located in the Holden laboratory at the University of Adelaide. The AWT, which is a low speed wind tunnel, whose outlet exhausts into a chamber of size $1.4 \times 1.4 \times 1.6$ m^3 and has a contraction outlet of 75 mm $\times$ 275 mm. The walls of the test chamber are acoustically treated with foam wedges to minimise reverberation. Owing to the small sized test section of the contraction outlet, the facility is best suited for scale model testing. The maximum flow velocity attainable in the AWT is restricted to ~ 38 m/s.

The finite length airfoil was fastened securely to one of the side plates of the housing with appropriate screws. The housing was then mounted to the flanges of the contraction outlet so that the leading edge of the airfoil was 50 mm away from the plane of the contraction outlet. The experimental setup with the infinite span airfoil in its test condition is shown in Figure 1. The finite length airfoil in its test arrangement is shown in Figure 2.

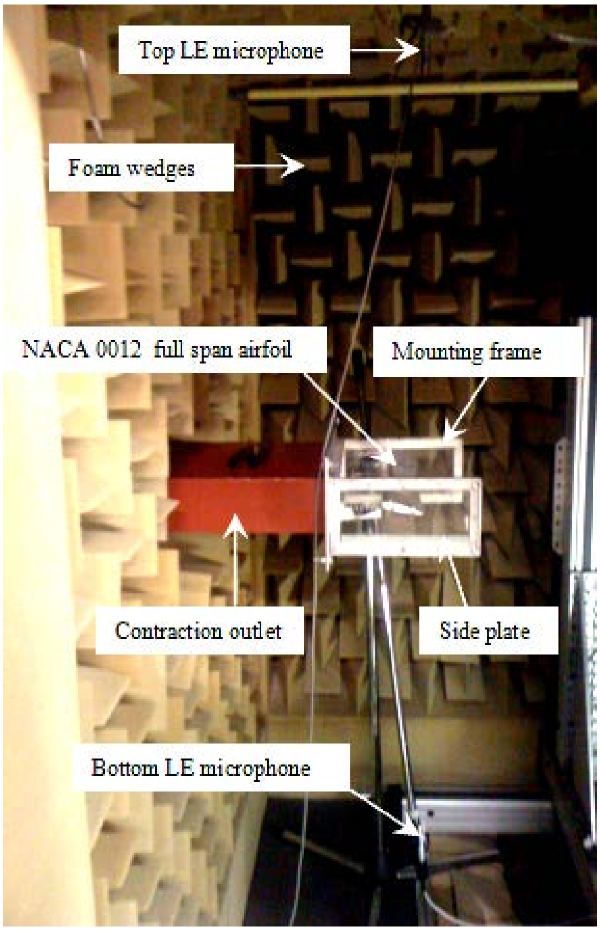

Figure 1: Experimental setup (α^* = 3.16º)

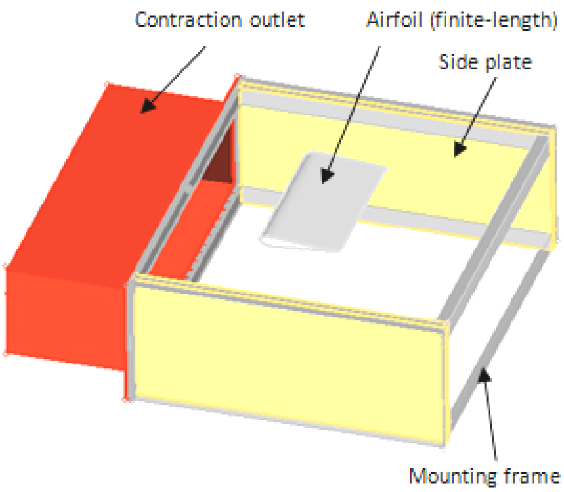

Figure 2: Airfoil in test condition (α^* = 0º)

Two phase matched B&K 1/2" microphones (Model # 4190) were mounted in the AWT chamber, one 560 mm directly above and another 560 mm directly below the trailing edge of the airfoil. Shear layer refraction (Amiet, 1978) was not taken into account. Both microphones were calibrated prior to taking airfoil self noise measurements. In order to eliminate wind noise created by the small movement of air in the test chamber outside of the test flow from the results, wind socks were placed on both microphones. A National Instruments data card interfaced with MATLAB data acquisition was used for collecting the microphone data. The data were converted from the time domain to the frequency domain using the Fast Fourier Transform. Microphone data were collected with a sampling rate of 2^{15} Hz for 8 seconds. The range of frequencies covered in the noise spectra is 200-14,894 Hz.

The first set of self noise measurements, using a finite length NACA 0012 airfoil (aspect ratio of 1.851 and chord of 67 mm), were made for 17 flow velocities from 5-38 m/s ($2.2 \times 10^4 < Re_c < 1.675 \times 10^5$) with 0º, 5º and 10º geometric angles of attack). Although Arcondoulis et al. (2009) presented acoustic analysis results for the corresponding full-span airfoil, for more meaningful comparison, a second set of noise measurements were made using a full-span NACA 0012 airfoil (aspect ratio of 4.105 and chord of 67 mm) for the same 17 flow velocities and three cases of angle of attack.

In order to compare the outcome of this study with experimental and numerical investigations carried out by others for similar geometries and flow conditions, a wind tunnel correction (Brooks et al., 1989) was applied to the angle of attack. This correction was applied to account for the flow curvature and downwash deflection of the incident flow caused by the finite size contraction outlet. Upon application of the wind tunnel correction, 0º, 5º and 10º geometric angles of attack became 0º, 1.58º and 3.16º true angles of attack (α^*) respectively (Arcondoulis et al., 2009).

RESULTS AND DISCUSSION

With the airfoil mounting frame fastened to the contraction outlet and background noise data were measured at static condition (ambient) and for flow velocities of 5-38 m/s. From the ambient noise (microphone self noise) and background noise spectra at flow speed of 38 m/s shown in Figure 3, it is evident that there are two peaks, one at 200 Hz (ambient noise) and the other at 300 Hz (background noise at 38 m/s). These peaks are due to low frequency noise from electronic equipment in the laboratory. Above 7500 Hz, the noise magnitude is very low. Therefore, the data were band passed from 200 - 7500 Hz and the data from 500 - 6000 Hz was analysed.

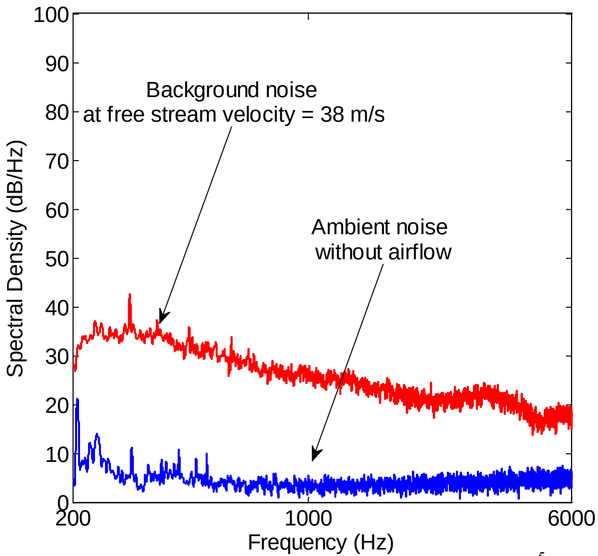

Figure 3: Background noise at $Re_c = 1.67 \times 10^5$ (flow velocity 38 m/s)

Although two microphones were used, the spectra from both microphones were similar. Therefore, the top microphone data were processed for acoustic analysis. Only for verification of the trailing edge as the major noise source and tip effects on noise generation, were the data obtained from both the upper and lower microphones used.

NOISE SOURCES

Brooks et al. (1989) used trailing edge noise scaling based on the theory presented by Ffowcs Williams and Hall (1970). The primary equation used for trailing edge noise scaling is

$$p^2 \propto \rho_0{}^2 v'^2 \frac{U_c^3}{c_0}\left(\frac{Ll}{r^2}\right)D, \qquad (1)$$

where p^2 is the mean square sound pressure at the observer located at a distance r from the trailing edge. The density of the medium is ρ_0, v'^2 is the mean-square turbulence velocity, U_c is the convective velocity, c_0 is the speed of sound, L is the span-wise extent wetted by the flow, l is the characteristic turbulence correlation scale and D is the directivity factor.

The noise spectra measured in the present experiments for the complete Reynolds number range and three cases of angle of attack for the finite length airfoil follow the same trend as the full span airfoil experimental data presented by Arcondoulis et al. (2009) for similar flow conditions. Noise spectra obtained for both airfoils at 0° angle of attack and $\mathrm{Re_c} = 1.1 \times 10^5$ (flow velocity 25 m/s) are shown in Figure 4.

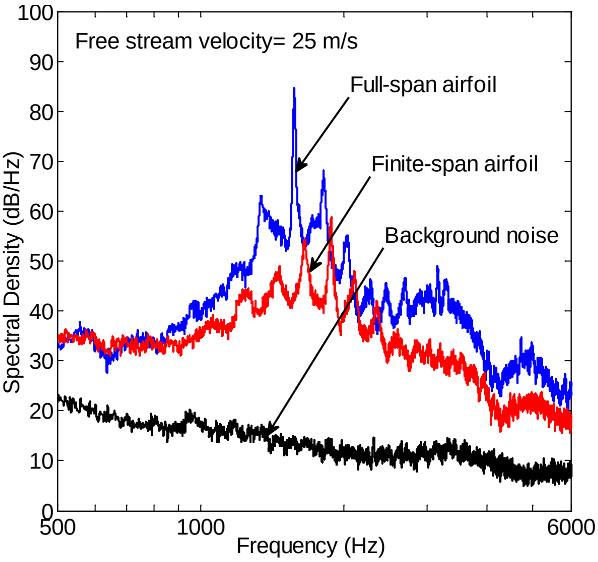

Figure 4: Noise spectra at $\mathrm{Re_c} = 1.1 \times 10^5$

From the acoustic analysis of the present experimental data for both airfoils at the same Reynolds numbers, it is evident that noise magnitudes of the primary tone and narrowband peaks are higher for the full span airfoil (aspect ratio of 4.105) when compared to those of the finite span airfoil (aspect ratio of 1.851). As all other parameters except span L are the same for both cases, according to equation (1), the ratio of p^2 for the full-span and finite-span airfoils should be ~ 2.28. Using the measured noise data for both airfoils at $\mathrm{Re_c} = 1.1 \times 10^5$ and $\alpha^* = 0°$, mean square average sound pressures (p^2) were calculated and the ratio of mean square sound pressure of the full span airfoil $\left(p_{fs}^2\right)$ to that of the finite span airfoil $\left(p_{fl}^2\right)$ was calculated to be 1.6.

Similarly, the ratio $\left(p_{fs}^2 / p_{fl}^2\right)$ for $2.2 \times 10^4 < \mathrm{Re_c} < 1.675 \times 10^5$ at various angles of attack were computed.

$$\left(p_{fs}^2 / p_{fl}^2\right) = 1.2 \text{ to } 1.6 \quad \text{at } \alpha^* = 0°,$$
$$= 1.4 \text{ to } 1.78 \text{ at } \alpha^* = 1.58° \text{ and}$$
$$\approx 1.0 \quad \text{at } \alpha^* = 3.16°$$

The above calculations suggest that the airfoil tip may be a significant noise source.

Blake (1986) has offered a widely accepted technique for isolating the trailing edge noise based on its characteristics. Kunze et al. (2002) and Moreau et al. (2010) have successfully applied adaptations of this technique for the acoustic analysis of various airfoil shapes for a wide variety of Reynolds numbers. As per the trailing edge noise characteristics, the top and bottom microphone noise data must be well correlated, equal in magnitude and opposite in phase.

The phase difference between the noise signals measured with the top and bottom microphones at a flow velocity of 38 m/s ($\mathrm{Re_c} = 1.675 \times 10^5$) and $\alpha^* = 0°$, 1.58° and 3.16° for both airfoils are shown in Figure 5.

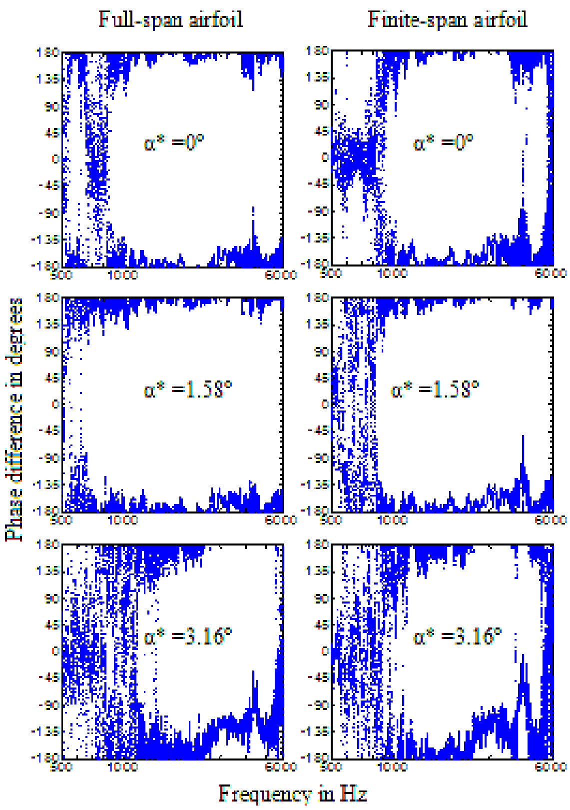

Figure 5: Phase difference between top and bottom microphone noise data at $\mathrm{Re_c} = 1.675 \times 10^5$

From the phase difference plots (Figure 5), it is evident that the majority of the noise generated by the finite-length airfoil, within the frequency band 800-5000 Hz is ~180° out of phase, consistent with airfoil self noise. Hence, the tip noise must be radiating in a similar manner to trailing edge noise.

ANALYSIS OF NOISE SPECTRA

True angle of attack (α^*) = 0°

For both the full span and finite-length airfoils, at Reynolds numbers from 2.2×10^4 to 4.0×10^4, although there is a broadband hump at low frequencies, the noise magnitudes are less than 20 dB and at higher frequencies the self noise of the airfoil is almost equivalent to the background noise. Therefore, results for these flow cases are not discussed here.

At $Re_c = 4.35 \times 10^4$ (flow velocity 10 m/s), audible tones were present. A broadband hump overlapped with narrowband peaks at lower frequencies is observed in the noise spectra for both full-span and finite-span test cases. In this particular flow case, the noise magnitude of the primary peak is around 35 dB which is well above the background noise (10 dB).

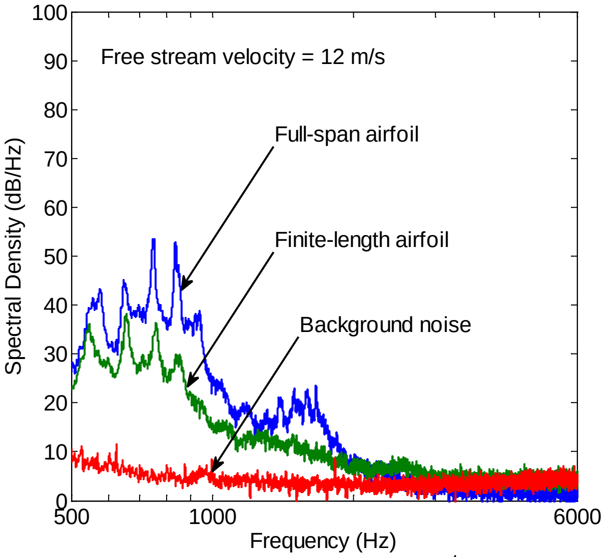

Figure 6: Noise spectra at $Re_c = 5.26 \times 10^4$ ($\alpha^* = 0°$)

At approximately $Re_c = 5.26 \times 10^4$ (Figure 6), distinct tones were measured and the broadband hump became significant with equidistant secondary peaks on both sides of the primary tone. With the increase in flow speed (Reynolds number), the noise magnitude of the tones increased and the broadband hump moved upwards in frequency. The noise spectrum for $Re_c = 8 \times 10^4$ (flow velocity 18 m/s) along with the background noise spectrum is shown in Figure 7.

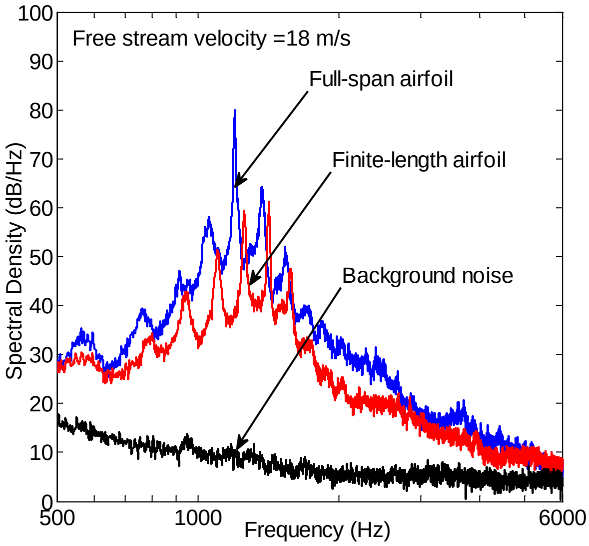

Figure 7: Airfoil self noise at $Re_c = 8 \times 10^4$ ($\alpha^* = 0°$)

For both airfoils at $Re_c \geq 1.315 \times 10^5$, a wider broadband hump with narrowband peaks of lesser magnitude and a secondary broadband hump were observed. Measured microphone data for the flow case of 33 m/s ($Re_c = 1.31 \times 10^5$ and $\alpha^* = 0°$) is shown in Figure 8. For every case at $\alpha^* = 0°$, it is evident that primary tones and narrowband peaks were higher in magnitude and lower in frequency for the full-span airfoil than those obtained for the finite-length airfoil.

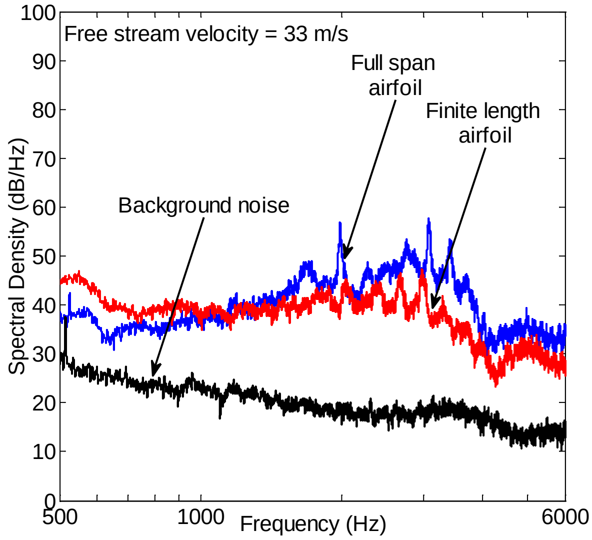

Figure 8: Noise spectrum at $Re_c = 1.31 \times 10^5$ ($\alpha^* = 0°$)

True angle of attack (α^*) = 1.58°

The following were observed from the acoustic measurements.

- For $2.2 \times 10^4 < Re_c < 1.675 \times 10^5$, noise spectra obtained for both airfoils at $\alpha^* = 1.58°$ exhibited the same trend (overall shape) when compared with those measured for $\alpha^* = 0°$.
- For all test cases below $Re_c = 6.2 \times 10^4$, the noise magnitudes of the tones and secondary narrowband peaks were slightly higher than those measured for 0° angle of attack. There was also an increase in the frequencies of tones when compared with the tonal frequencies at 0° angle of attack. Magnitudes of the tones and narrowband peaks for full span airfoil were higher while frequencies of tones and peaks were higher for finite-length airfoil (Figure 9).

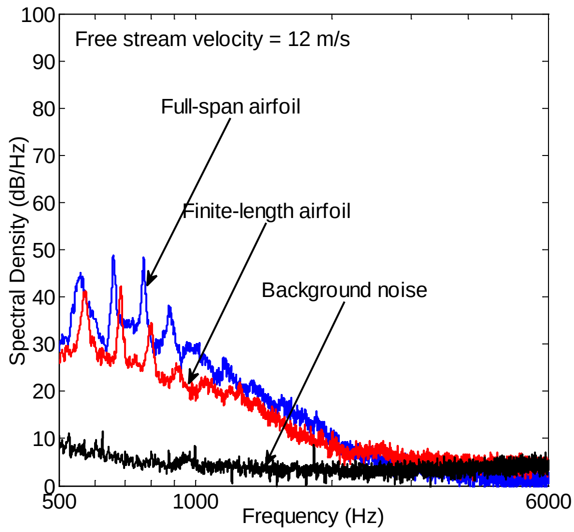

Figure 9: Noise spectra for $Re_c = 5.26 \times 10^4$ ($\alpha^* = 1.58°$)

- For the finite-length airfoil, for all test cases within 6.2×10^4 <Re_c< 1.0×10^5 (Figure 10), along with the increase in tonal frequencies, the magnitudes of the tones and narrowband secondary tones were lower than those measured at 0º angle of attack. In the case of the full span airfoil, noise magnitudes are higher at 0º angle of attack and the frequency of the tones are higher for 1.58º angle of attack (Figure 11).

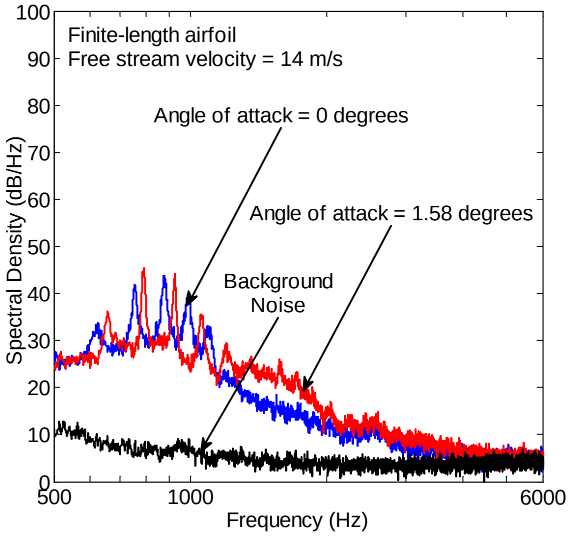

Figure 10: Noise spectra at $Re_c = 6.14\times 10^4$

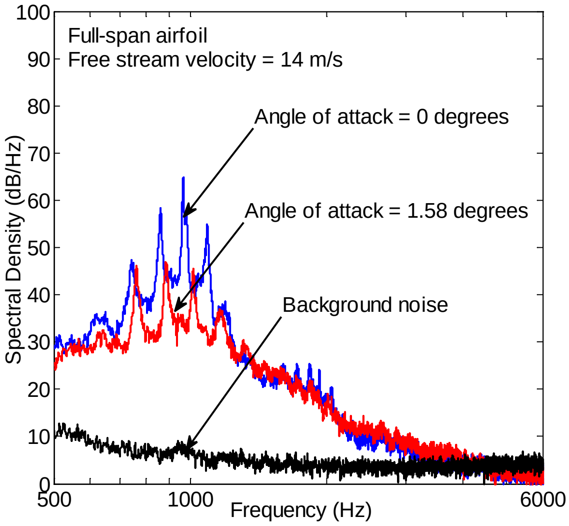

Figure 11: Noise spectra at $Re_c = 6.14\times 10^4$

- For both airfoils, at 1.0×10^5<Re_c<1.67×10^5 (Figures 12 and 13), tones were dominant, more pronounced and higher in magnitude when compared to those at 0º angle of attack.

True angle of attack (α*) = 3.16º

The noise spectra at 3.16º angle of attack and Re_c = 1.18×10^5 and 1.67×10^5 are shown in Figures 14 and 15, respectively.

From the noise measurements at 2.2×10^4<Re_c< 1.67×10^5, the following observations were made.

- Noise data obtained using the finite-length airfoil (Figures 14 and 15) were purely broadband in nature without any tonal components or narrow band peaks. Noise spectra were also without any broadband humps as observed in the former two cases of angle of attack. The noise magnitude at all frequencies is less than 40 dB and at least 20 dB more than that of the background noise levels for experiments at $Re_c = 1.0\times 10^5$ - 1.67×10^5.

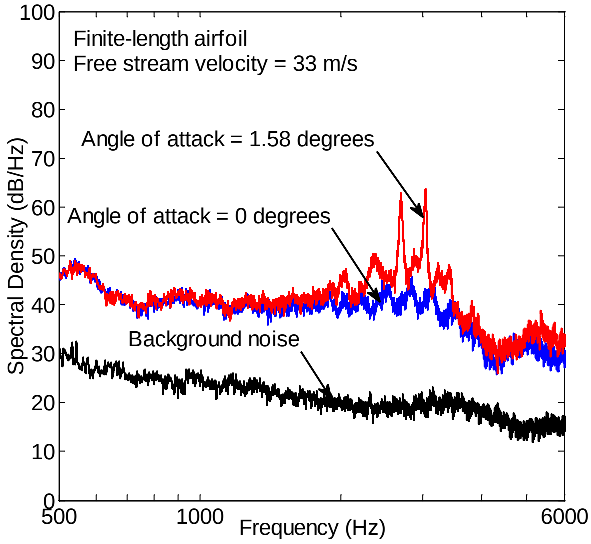

Figure 12: Noise spectra at $Re_c = 1.53\times 10^5$

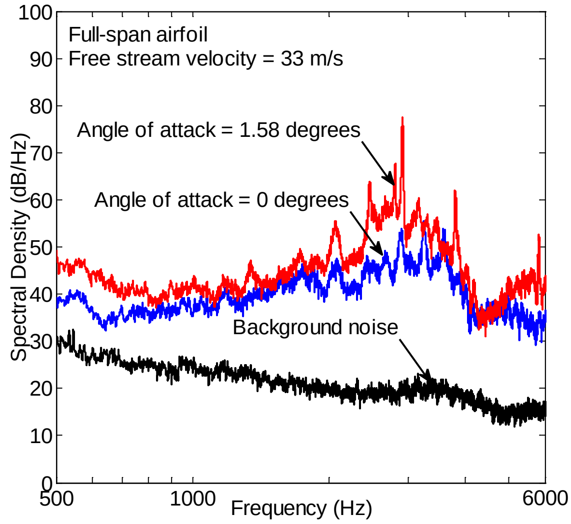

Figure 13: Airfoil noise spectra at $Re_c = 1.53\times 10^5$

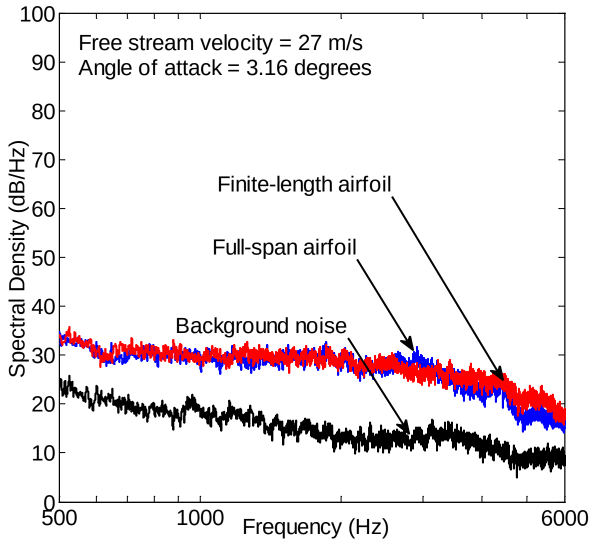

Figure 14: Noise spectra at $Re_c = 1.18\times 10^5$

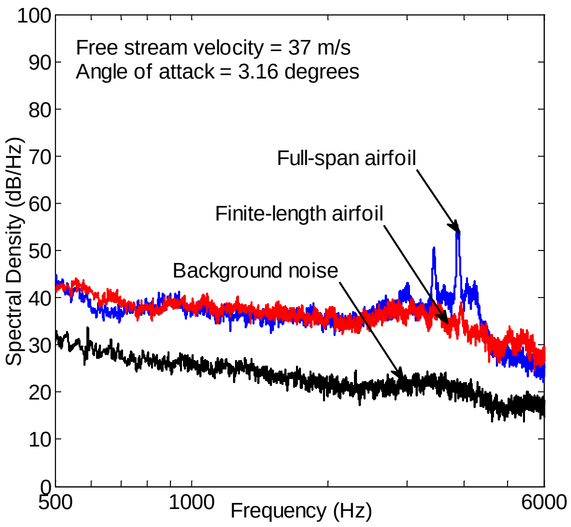

Figure 15: Noise spectra at Re_c 1.63×10^5

- For a full-span airfoil at 1.45×10^5 <Re_c<1.67×10^5, the radiated noise contatined pure tones and narrowband peaks with significant magnitude.

NOISE MAGNITUDE

Noise magnitudes for all 51 experimental cases of the finite span airfoil (aspect ratio of 1.851) are presented and discussed in this section.

Arcondoulis et al. (2009) have compared noise magnitudes at 1 kHz, 1.5 kHz and 2.5 kHz for the full span airfoil (aspect ratio of 4.105) at 5×10^4<Re_c<1.5×10^5. It is evident from the noise spectra of the present experiments, that there is an increase in the tonal noise frequencies from case to case. Therefore, measuring noise magnitude at a single frequency would not yield a meaningful value. Das et al. (2011) employed an average filtered FFT amplitude method when analyzing acoustic signatures. Here, in the region of tonal and narrowband peaks, the spectra were appropriately divided into frequency bands in such a way that every band contained a narrowband peak. The band root-mean-square (RMS) noise magnitude was then calculated and compared with other flow cases at 965 Hz, 1130 Hz, 1475 Hz, 2300 Hz, 2675 Hz mid-band frequencies in Figures 16-18.

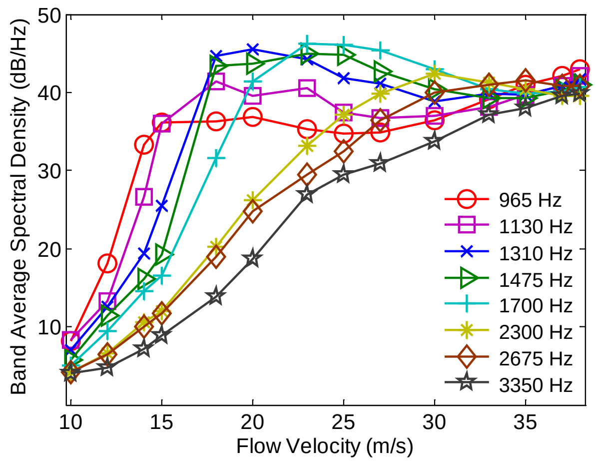

Figure 16: RMS of spectral density vs flow velocity (Finite-length airfoil at 0º angle of attack)

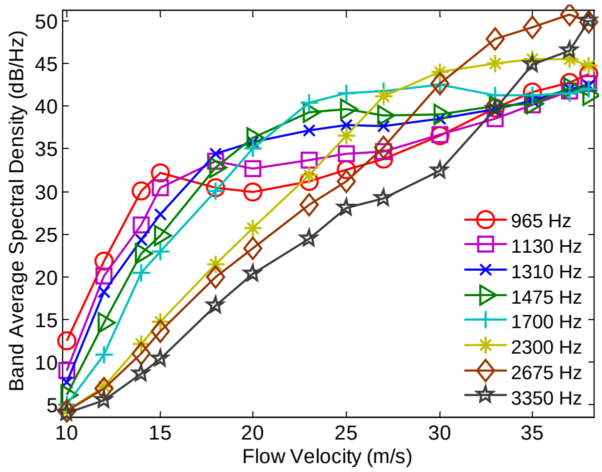

Figure 17: RMS of spectral density vs flow velocity (Finite-length airfoil at 1.58º angle of attack)

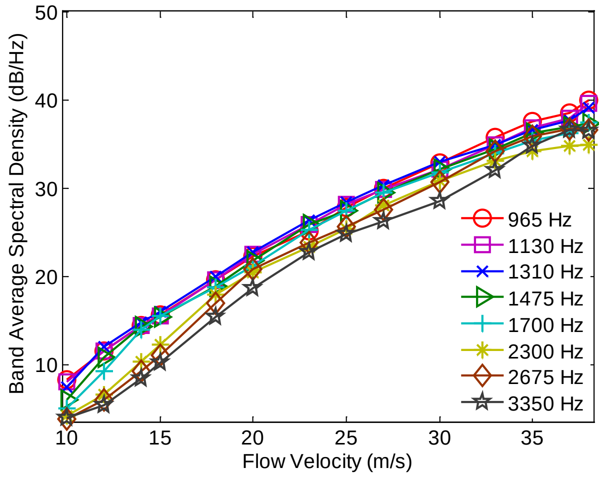

Figure 18: RMS of spectral density vs flow velocity (Finite-length aifoil at 3.16º angle of attack)

From Figures 16-18, it is evident that the noise magnitudes are greatest at 0º angle of attack at all flow velocities less than 30 m/s. At α* = 3.16º, the variation of the band RMS spectral density is almost linear for all of the frequency bands (Figure 18).

FREQUENCY BEHAVIOR

Paterson et al. (1973) have measured far-field noise and airfoil surface fluctuations for NACA 0012 airfoils and observed the presence of discrete tones. They estimated the frequency dependence of the discrete tonal noise on the velocity and chord of the airfoil to be

$$f = 0.011\frac{U^{1.5}}{\sqrt{C\upsilon}}, \qquad (2)$$

where U is the free-stream velocity, C is the chord of the airfoil and υ is the dynamic viscosity of the medium.

Tam (1974) carried out further investigations on the discrete tonal behavior of noise radiated from the isolated airfoil and showed that experimental results were in agreement with the quantitative deductions based on a feedback loop model. Experimental investigations by Arbey et al. (1983) are also in agreement with the tonal frequency scaling law in Equation 2. For certain ranges of Reynolds numbers, tonal frequencies followed the power laws of the form $f \propto U^{1.5}$ and equidistant secondary tonal peaks followed the power law of the form $f \propto U^{0.85}$.

Tonal frequencies were plotted against the flow velocity from the experimental results for 17 flow velocities and two cases of airfoil true angles of attack 0º and 1.58º. The plots are shown in Figures 19 and 20. From these figures it is evident that, up to certain range of Reynolds numbers ($3.95\times10^4 < Re_c < 6.58\times10^4$), tonal frequency ($f$) followed power law of a form $f \propto U^{1.6}$ and later ($7.9\times10^4 < Re_c < 1.67\times10^5$) followed the power law $f \propto U^{0.9}$. The overall (primary and secondary peaks together) trend followed the power law $f \propto U^{1.22}$. The results are in good agreement with those presented by Arbey et al. (1983). Takashi et al. (2009) did similar experimental studies to investigate the tonal behavior and its frequency selection, but their research outcome is not used for comparison here as a NACA 0015 airfoil was used for their experimental study.

Figure 21 shows the frequencies of the tones measured in this study compared with those measured in the studies by Paterson et al. (1973), Nash et al. (1999), Desquenses et al. (2007) and Arcondoulis et al. (2009). It is evident that tones for the cases of 0º and 1.58º angles of attack were in good agreement with the tonal envelope generated by Nash et al. (1999). For 3.16º angle of attack, the results were not in good agreement with the tonal envelope. It is important to note that tonal envelope presented by Nash et al. (1999) is based on a semi-empirical relationship.

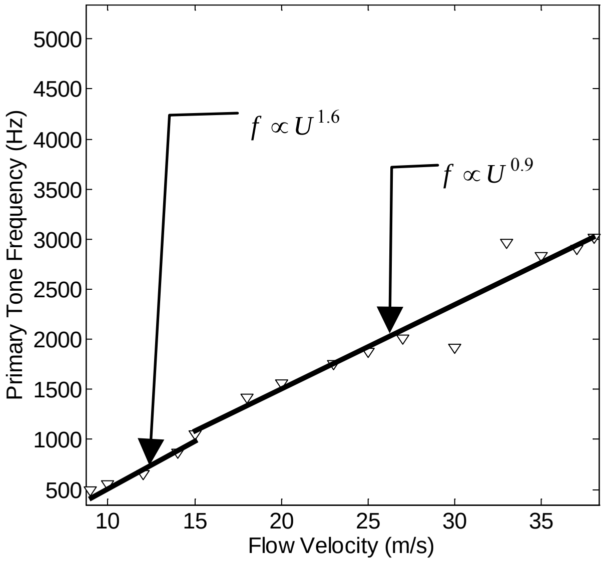

Figure 19: Frequency of the primary tones vs flow velocity for airfoil at $\alpha^* = 0º$

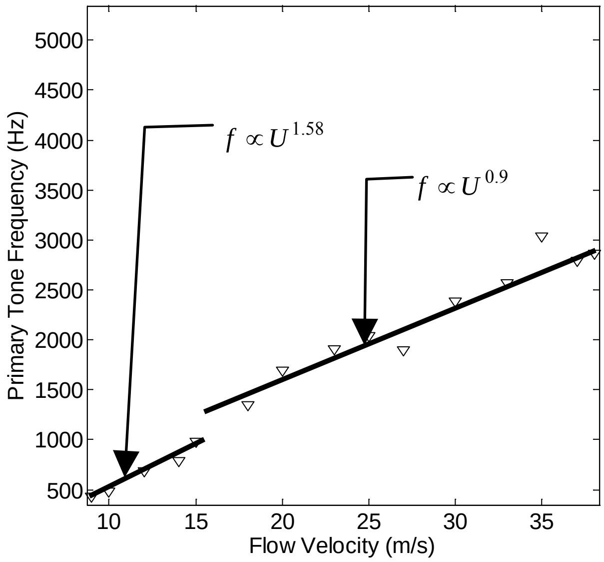

Figure 20: Frequency of the primary tones vs flow velocity for airfoil at $\alpha^* = 1.58º$

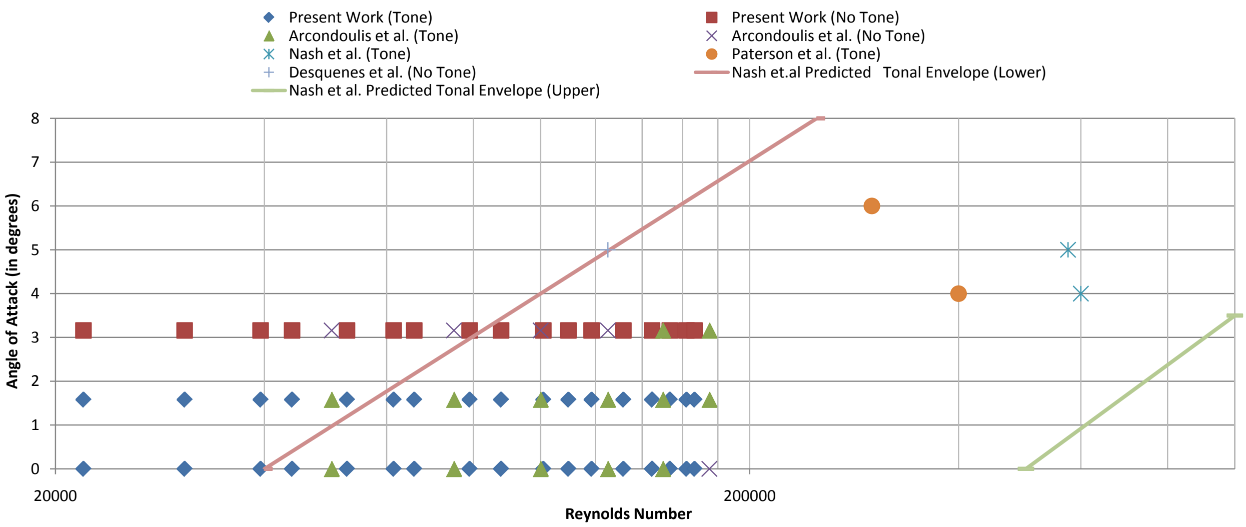

Figure 21: Tonal envelope predicted by Nash et al.(1999)

CONCLUSION

This paper has presented results of an experimental study on the noise produced by two NACA 0012 airfoils: one is a finite-length (aspect ratio of 1.851) airfoil and the other is a full-span (infinite length with an aspect ratio of 4.105) at Reynolds numbers ($2.2 \times 10^4 < Re_c < 1.675 \times 10^5$) and three angles of attack ($\alpha^* = 0°$, 1.58 and 3.16°).

The purpose of the present experimental study was to gain insight into the tip effects on the generated noise and also on how a finite wing produces tonal noise and how this differs to a full-span airfoil. The following conclusions were drawn from the airfoil self noise measurements.

1. For the whole range of Reynolds numbers considered ($2.2 \times 10^4 < Re_c < 1.675 \times 10^5$) and at $\alpha^* = 0°$, 1.58° and 3.16°, the results indicate that tip noise is significant.
2. Tip noise characteristics are consistent with trailing edge noise.
3. The tip effect is predominant at $\alpha^* = 3.16°$ when compared to $\alpha^* = 0°$ and 1.58°. Overall, noise generated by the finite-length airfoil (aspect ratio of 1.851) was almost equivalent to the noise generated by the full-span airfoil (aspect ratio of 4.105).
4. For the finite-length airfoil, tonal components at $\alpha^* = 1.58°$, in comparison with those at 0° angle of attack, were greater in magnitude at lower Reynolds numbers ($Re_c < 6.2 \times 10^4$). For all other flow cases within $6.2 \times 10^4 < Re_c < 1.0 \times 10^5$, the level of the tonal components were reduced in magnitude. In the Reynolds numbers range $1.0 \times 10^5 < Re_c < 1.67 \times 10^5$, pure tones were observed that had significantly higher levels when compared to those obtained at $\alpha^* = 0°$.
5. For both airfoils at $\alpha^* = 0°$ and 1.58°, tones were observed at all Reynolds numbers. At higher Reynolds numbers ($Re_c \geq 1.315 \times 10^5$), tones were lesser in magnitude and higher in frequency.
6. At $\alpha^* = 3.16°$, no tones were observed for the finite-length airfoil and for the full-span airfoil, tones were observed for all measurements at $Re_c \geq 1.32 \times 10^5$.
7. The frequency of the primary tones produced by the finite-length airfoil at $\alpha^* = 0°$ and 1.58° followed the power laws;

$$f \propto U^{1.6} \text{ at } 2.2 \times 10^4 < Re_c < 8.0 \times 10^4$$

$$f \propto U^{0.9} \text{ at } 8.0 \times 10^4 < Re_c < 1.675 \times 10^5$$

8. The frequency of the primary and secondary tones produced by finite-length airfoil at $\alpha^* = 0°$ and 1.58° followed a power law:

$$f \propto U^{1.22} \text{ at } 2.2 \times 10^4 < Re_c < 1.675 \times 10^5$$

The authors aim to further investigate the finite length airfoil noise-producing mechanisms in more detail and it is anticipated that the individual and relative effects of the leading edge, trailing edge and tip will be examined. With the help of flow velocity measuring techniques, tip effects will also be studied in greater detail by varying the aspect ratio of the airfoil.

REFERENCES

Amiet, R. 1978, 'Refraction of Sound by a Shear Layer', *Journal of Sound and Vibration*, Vol. 58, No. 4, pp. 462-482.

Arbey, H. and Bataille, J. 1983, 'Noise generated by airfoil profiles placed in a uniform laminar flow', *Journal of Fluid Mechanics,* Vol. 134. pp. 33-47.

Arcondoulis, EJG. Doolan, CJ. and Zander, AC. 2009, 'Airfoil Noise Measurements at Various Angles of Attack and Low Reynolds Number', *Proceedings of ACOUSTICS 2009,* Adelaide, Australia.

Blake, WK. 1986, Mechanics of Flow Induced Sound and Vibration, volume I and II. Academic Press, London, UK.

Brooks, TF. Pope, DS. and Marcolini, MA. 1989, 'Airfoil Self-Noise and Prediction', NASA Reference Publication 1218.

Das, SP. Das, DP. Behera, SK. and Mishra, BK. 2011, 'Interpretation of mill vibration signal via wireless sensing', *Mineral Engineering,* Vol. 24, pp. 245-251.

Desquesnes, G., Terracol, M. and Sagaut, P. 2007, 'Numerical investigation of the tone noise mechanism over laminar airfoils', *Journal of Fluid Mechanics,* Vol. 591, pp. 155-182.

Doolan, CJ. 2008, 'A review of airfoil trailing edge noise and its prediction' *Acoustics Australia*, Vol. 36, pp. 7-13.

DOT/FAA *Noise Standards: Aircraft type and airworthiness certification*, FAR part 36, January 1, 1990.

Ffowcs-Williams, J. and Hall, L. 1970, 'Aerodynamic sound generation by turbulent flow in the vicinity of a scattering half plane', *Journal of Fluid Mechanics*, Vol. 40, No. 4, pp. 657-670.

Kingan, M. and Pearce, J. 2009, 'Laminar boundary layer instability noise produced by an aerofoil', *Journal of Sound and Vibration*, Vol. 322, pp. 808-828.

Kunze, C. Lynch III, DA. and Mueller, TJ. 2002, 'Effect of trailing edge geometry on vortex shedding and acoustic radiation', *8th AIAA/CEAS Aeroacoustics Conference,* AIAA 2002-2435.

Moreau, DJ. Tetlow, MR. Brooks, LA. and Doolan, CJ. 2010 'Acoustic analysis of flat plate trailing edge noise', *Proceedings of 20th International Congress on Acoustics,* Sydney, Australia.

Nash, E., Lowson, M. and McAlpine, A. 1999, 'Boundary-layer instability noise on aerofoils', *Journal of Fluid Mechanics,* Vol. 382, pp. 27-61.

Paterson, R., Vogt, P., Fink, M. and Munch, C. 1973, 'Vortex Noise of Isolated Airfoils', *J.Aircraft*, Vol. 10, No. 5, pp. 296-302.

Smith, MJT. 1989, Aircraft Noise, Cambridge Aerospace Series, Cambridge University Press, Cambridge.

Takashi, A. Marthijn, T. and Shohei, T. 2009, 'Airfoil Tonal Noise Generation in Resonant Environments', *Transactions of the Japan Society of Aeronautical and Space Sciences*, Vol. 52, No.176, pp. 74.

Tam, C. 1974, 'Discrete Tones of isolated airfoils', *Journal of the Acoustic Society of America*, Vol. 55, No. 6, pp. 1173-1177.